The Use of Cyclometalated NHCs and Pyrazoles for the Development of Fully Efficient Blue PtII Emitters and Pt/Ag Clusters

Lorenzo Arnal,[b] Sara Fuertes*,[b] Antonio Martín,[b] and Violeta Sicilia*[a]

[a] *Departamento de Química Inorgánica, Escuela de Ingeniería y Arquitectura de Zaragoza, Instituto de Síntesis Química y Catálisis Homogénea (ISQCH), CSIC - Universidad de Zaragoza, Campus Río Ebro, Edificio Torres Quevedo, 50018, Zaragoza (Spain). E-mail: sicilia@unizar.es.*

[b] *Departamento de Química Inorgánica, Facultad de Ciencias, Instituto de Síntesis Química y Catálisis Homogénea (ISQCH), CSIC - Universidad de Zaragoza, Pedro Cerbuna 12, 50009, Zaragoza (Spain). E-mail: sfuertes@unizar.es.*

Abstract: New bis-pyrazole complexes $[Pt(C^C^*)(RpzH)_2]X$, containing a cyclometalated N-heterocyclic carbene ligand (HC^C* = 1-(4-(ethoxycarbonyl)phenyl)-3-methyl-1*H*-imidazol-2-ylidene) were prepared as chloride (X = Cl^-, RpzH: 3,5-Me_2pzH **1a**, 4-MepzH **2a**, pzH **3a**), perchlorate (X = ClO_4^-,**1b – 3b**), or hexafluorophosphate (X = PF_6^-, RpzH: 3,5-Me_2pzH **1c**) salts. The X-ray structure of **1a** showed that the Cl^- anion is trapped by the cation through two N-H···Cl bonds. This cation-anion association is kept in solution, being responsible of both, the low value of the molar conductivity of **1a** in acetone and the high downfield shift of the N-H NMR resonance when compared to those of **1b** and **1c**. The low lying absorption and the emission bands were assigned to intraligand (ILCT) charge transfer on the NHC group. Quantum yield measurements revealed that some of these compounds are amongst the most efficient blue-light emitters, with values up to 100%. Proton abstraction from the coordinated 3,5-Me_2pzH in **1b** by NEt_3 and replacement by Ag^+ afforded a neutral $[Pt_2Ag_2]$ cluster containing Pt → Ag dative bonds.

Introduction

Cyclometalated N-heterocyclic carbenes (NHCs) have revealed as promising groups to get efficient and stable phosphorescent transition metal complexes.[1] Presence of two strong carbon-metal bonds confers robustness and stability and may provide long-term functional materials.[2] In the chemistry of Pt(II) they also induce high crystal field splitting, therefore reducing the photo- or thermal population of high-lying metal dd* states, which result in non-radiative deactivation and degradation via bond-breaking processes.[3] Since population of a high energy excited state is required for an efficient blue emission, the incorporation of strong field ligands such as NHCs is essential in the design of efficient blue-emitting compounds.[2d, 2e, 2h-j] Moreover, the use of bidentate cyclometalated NHCs ligands allows the emission tunability of the Pt(II) complexes by varying either, the substituents in the NHC or the nature of the ancillary groups.[1d, 4] As an example, our precedent work showed that Pt(II) compounds containing cyclometalated N-heterocyclic carbenes (chart 1) resulted to be efficient emitters in the blue - yellow region of the visible spectra.[4]

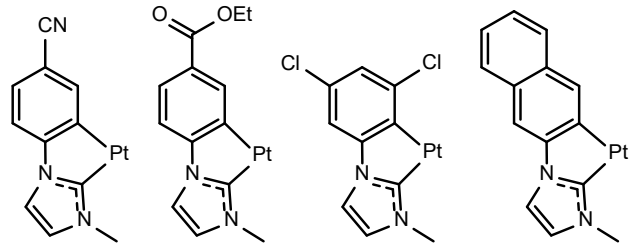

Chart 1. Overview of Reported Cycloplatinated NHC Based Motifs

Furthermore, it is well known the interest of pyrazole (RpzH) complexes in fields such as medicine, since cis-dichlorobis(pyrazole)platinum(II)[5] and related compounds were proven to have anticancer activity.[6] Pyrazole-based complexes are also useful in

catalysis, in hydrogenation and transfer hydrogenation processes through metal-ligand bifunctional cooperation.[7] Moreover, mononuclear pyrazole complexes are of interest in molecular architecture and luminescence. Pt(II) complexes such as, $[Pt(C{\equiv}CPh)_2(RpzH)_2]$,[8] $[Pt(C\hat{}N)(RpzH)_2](PF_6)$,[9] $[Pt(N\hat{}N)(RpzH)_2](PF_6)_2$,[9a] $[PtCl(3,5\text{-}Ph_2pzH)_3]Cl$, $[PtCl(3,5\text{-}Ph_2pz)(3,5\text{-}Ph_2pzH)_2]$, $[Pt(3,5\text{-}Ph_2pz)(3,5\text{-}Me_2pzH)(3,5\text{-}Ph_2pzH)_2]Cl$,[10] and $[Pt(3,5\text{-}Me_2pzH)_4]Cl_2$[11] are easily deprotonated and have been used as synthons for the synthesis of a great variety of homo- and hetero-polynuclear ($[PtM_2]$, $[Pt_2M_2]$, M= Ag, Au) compounds. The 1,2-dihaptobridging Rpz ligands can hold metal atoms in close proximity while permitting a wide range of structures and intermetallic separations, with the strength of the metallophilic interactions affecting the emissive properties.[8-9]

Keeping in mind the above mentioned, we decided to expand our work[4] to pyrazole complexes, to combine the robustness of the cyclometalated NHCs Pt(II) chromophores and the structural versatility of RpzH ligands to achieve new stable and efficient photoluminescent compounds. As a result, we got the new mononuclear bis-pyrazole complexes $[Pt(C\hat{}C^*)(RpzH)_2]X$, containing a cyclometalated NHC ligand (HC^C* = 1-(4-(ethoxycarbonyl)phenyl)-3-methyl-1*H*-imidazol-2-ylidene). They were isolated as chloride (Cl^-), perchlorate (ClO_4^-) or hexafluorophosphate (PF_6^-) salts, being possible because of the availability of $[\{Pt(C\hat{}C^*)(\mu\text{-}Cl)\}_2]$(**A**)[4b] as starting material. Here we describe their synthesis, characterization and photophysical properties, explained in some cases with the aid of theoretical calculations (TD and DFT). Some of these compounds resulted to be very efficient blue emitters with photoluminescent quantum yield (PLQY) up to 100%. The replacement of the proton in the coordinated pyrazoles of $[Pt(C\hat{}C^*)(3,5\text{-}Me_2pzH)_2]ClO_4$ by Ag^+ allowed us to get a heteronuclear $[Pt_2Ag_2]$ cluster and its luminescent properties have been compared with those of its precursor.

Results and Discussion

Synthesis and characterization of mononuclear bis-pyrazole Pt(II) compounds

The new bis-pyrazole complexes $[Pt(C\hat{}C^*)(RpzH)_2]^+$, containing a cyclometalated N-heterocyclic carbene ligand (HC^C* = 1-(4-(ethoxycarbonyl)phenyl)-3-methyl-1*H*-imidazol-2-ylidene) were prepared and isolated as the chloride (X = Cl^-, RpzH: 3,5-Me_2pzH **1a**, 4-MepzH **2a**, pzH **3a**), perchlorate (X = ClO_4^-,**1b – 3b**), or hexafluorophosphate (X = PF_6^-, RpzH: 3,5-Me_2pzH **1c**) salts following the strategies indicated in Scheme 1.

Compounds **1a**, **2a** and **3a** were prepared by treatment of a suspension of **A** with 4.4 equivalents of the corresponding pyrazole ligand (RpzH) in acetone at room temperature (see Scheme 1 path a).

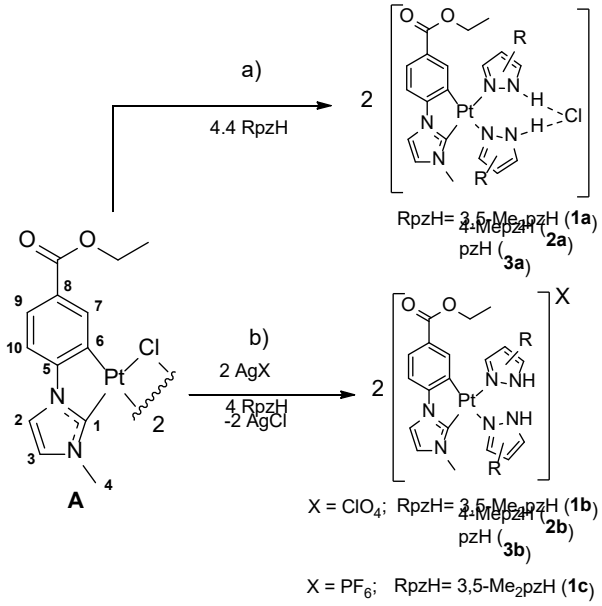

Scheme 1. Numbering scheme and synthetic pathways

They were obtained from their solutions as pure solids in moderately good yield (61% **1a**, 64% **2a**, 60% **3a**) and fully characterized (see Experimental Section and Figures 1 and S1 – S9). The proposed stoichiometry for them was later confirmed by single crystal X-ray diffraction of **1a** (see below Figure 1). In solution, the ^{1}H NMR spectrum

in CD_2Cl_2 of **1a** (Figure S1) shows one set of signals corresponding to the C^C* group and two non-equivalent 3,5-Me_2pzH ligands. However the ^{1}H NMR spectra of **2a** and **3a** (Figures S3 and S4 (top)) showed the additional presence of the corresponding species [PtCl(C^C*)(RpzH)](**B**). Species **B** result also from the reaction of **A** with 2 equiv. of RpzH. The *cis*-(C*,Cl) and *trans*-(C*,Cl) isomers appeared in a ratio 14:1 and 16:1 for 4-MepzH and pzH respectively (see Figure S8) and were identified on the bases of the ^{1}H NMR.[12] Species **B** would be formed from **2a**/**3a** by displacement of a RpzH ligand by the Cl^-, and co-exist in solution with **2a**/**3a** in a dynamic equilibrium, such as the represented in Scheme 2. In agreement with this, addition of 4-MepzH/pzH to a solution of compound **2a/3a** in CD_2Cl_2 shifts this equilibrium to the left and the signals attributed to **B** disappear (see Figures S3/S4 bottom).

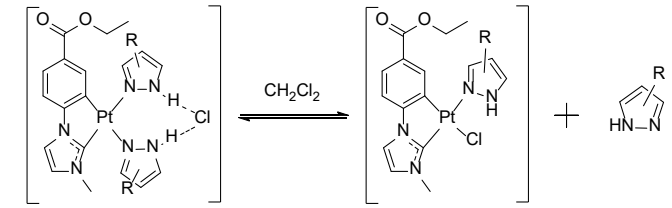

Scheme 2. Dynamic equilibria of **2a** and **3a** in CH_2Cl_2 solution at r.t. For **B** the major isomer is just represented.

Variable temperature ^{1}H NMR studies, carried out in CD_2Cl_2, for **2a** and **3a** showed that as the temperature decreases the amount of **B** decreases, in such a way that **2a** and **3a** are the only species in solution at temperatures equal or below 243 K and 223 K respectively (see Figures S5 and S6). Because the equilibrium represented in Scheme 2 becomes spontaneous ($\Delta G = \Delta H - T\Delta S < 0$) when the temperature raises and $\Delta S > 0$, the dissociation must be an endothermic process. The calculated values for ΔS (93.7 J k^{-1} mol^{-1} **2a**, 111.2 J k^{-1} mol^{-1} **3a**) and ΔH (ΔH= 26.5 KJ mol^{-1} **2a**, 30.3 KJ mol^{-1} **3a**)

confirmed these statements (Figure S9). These results illustrate the higher basicity of 3,5-Me_2pzH with respect to 4-MepzH and pzH in agreement with the pKa value of their conjugate acids (3,5-Me_2pzH: 4.06, pzH: 2.83).[10]

The molecular structure of **1a**, determined from a single crystal X-ray diffraction study, showed the *cis* arrangement of the two 3,5-Me_2pzH-κN ligands in the mononuclear complex and the presence of the chloride anion joined to the cation through two N-H···Cl hydrogen bonds (see Figure 1).

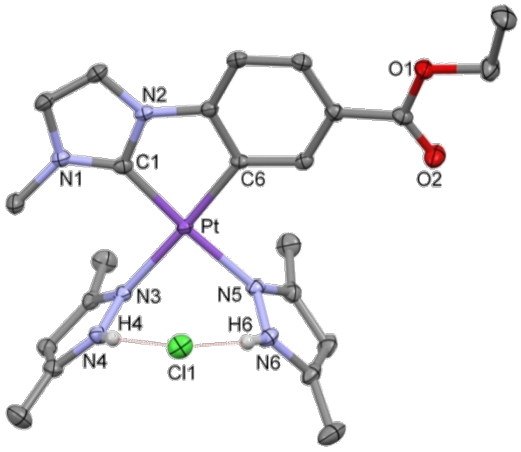

Figure 1. Molecular structure of **1a**. Ellipsoids are drawn at their 50% probability level; solvent molecules and hydrogen atoms were omitted for clarity. Selected bond lengths (Å) and angles (º) for **1a·CH_2Cl_2**: Pt(1)-C(1) = 1.964(3); Pt(1)-C(6) = 2.003(2); Pt(1)-N3 = 2.100(2); Pt(1)-N5 = 2.077(2); C(1)-Pt-C(6) = 80.17(10); C(6)-Pt-N(5) = 95.49(9); C(1)-Pt-N(3) = 96.76(9); N(5)-Pt-N(3) = 87.55(8).

The small bite angle of the cyclometalated ligand [80.17(10)º] together with the Pt–C6 and Pt–C1(C*) distances are similar to those found in other five membered metalocycles of Pt(II) with NHC ligands.[4a, 4d] These distances evidence the low *trans* influence of the 3,5-Me_2pzH ligands since them are shorter than those observed in complexes such as [Pt(NC-C^C*)(P^P)]PF_6 (P^P= diphenylphosphino-ethane)[12] and [Pt(R-C^C*)(C≡NR')$_2$]PF_6 (R = CN, CO_2Et; R'= Xyl, ^{t}Bu).[4b] The Pt-N bond distances

are rather long and similar to those found in complex *cis*-[Pt(C≡C)$_2$(Hdmpz)$_2$],[8] which is in agreement with the high *trans* influence of both C atoms (C1 and C6) of the EtO$_2$C-C^C*-κC,C* ligand, mainly the σ–bonded C$_{Ar}$(C6). The plane defined for the 5-membered metalocycle (Plane 1: Pt, C1, N2, C5, C6) is basically co-planar with the platinum coordination plane (Plane 2: Pt, C1, C6, N3, N5). However, the 3,5-Me$_2$pzH ligands are almost perpendicular to it with interplanar angles of 88.18(0.07)º and 80.34(0.06)º for planes 3 (N3, N4, C14-C16) and 4 (N5, N6, C19-C23) respectively, and they are also perpendicular one to another with the interplanar angle being 89.34(0.09)º. The two 3,5-Me$_2$pzH ligands trap the chloride anion through two N-H···Cl hydrogen bonds, with the H4-Cl1-H6 angle being 79.22(1.22)º, almost the theoretical value (90º) for the lone electron pairs of the chloride ligand. The parameters corresponding to both, the two H bonds show values typical for this kind of interaction (H4···Cl1 = 2.3164 (361) Å, N4-H4···Cl1 = 162.39º, H6···Cl1 = 2.2662 (356) Å, N6-H6 ···Cl1 = 171.9º).[13] This cation-anion association keeps in solution being the conductivity value of a $5\cdot10^{-4}$ M solution of **1a** in acetone (Λ_M: 9.53 Ω^{-1} cm^2 mol^{-1}) clearly lower that that expected for a 1:1 electrolyte (Λ_M: 100-120 Ω^{-1}cm^{2}mol^{-1}).[14]

In order to avoid the above analyzed chemical equilibria in solution and be able to study the optical properties of these new bis-pyrazole platinum complexes, we addressed their synthesis as salts of non-coordinating anions: ClO_4^- and PF_6^-. So, compounds **1b, 2b, 3b** and **1c** were prepared by treatment of a suspension of **A** with 2 equivalents of AgX (X= ClO_4 **1b – 3b**, PF_6 **1c**) and 4 equivalents of the corresponding RpzH ligand in acetone at room temperature (see Scheme 1 path b). The workup of their corresponding solutions allowed them to be obtained in good yield (71% **1b**, 89% **2b**, 78% **3b**, 45% **1c**) and be characterized (see Experimental Section and Figures S10-S18 in SI).

The strong IR absorptions due to ClO_4^- and PF_6^-anions for **1b-3b,** and **1c**; the corresponding $[Pt(C^C^*)(RpzH)_2]^+$ peak in their MALDI(+) mass spectra and their ^1H, $^{13}C\{^1H\}$ and $^{195}Pt\{^1H\}$ NMR spectra are in agreement with the proposed stoichiometry. For these compounds the NH resonances appear highfield shifted with respect to those of **1a** (see Figure S18 for **1a-1c**), most surely due to differences in the H-bond interactions with the counteranion. Taking into account that stronger interactions lead to higher downfield shifting,[15] the H-bond interactions are significantly stronger in **1a** (NH···Cl) than in **1b** (NH···O-ClO_3) and **1c** (NH···F-PF_5), which is in agreement with the conductivity values observed (9.53 Ω^{-1} cm^2 mol^{-1} (**1a**), 103.5 Ω^{-1} cm^2 mol^{-1} (**1b**), 134.8 Ω^{-1} cm^2 mol^{-1}(**1c**)). In spite of their similarities while **1b, 2b,** and **1c** are stable in CH_2Cl_2 solution at r.t., **3b** partially evolves to give $[\{Pt(C^C^*)(\mu\text{-}pz)\}_2]$ and free pzH. After one hour in CD_2Cl_2 the ratio **3b**: $[\{Pt(C^C^*)(\mu\text{-}pz)\}_2]$ was 8:1. Once again this result illustrates the lower basicity of pzH with respect to 3,5-Me_2pzH and to 4-MepzH.[10]

Reactivity of $[Pt(C^C^*)(3,5\text{-}Me_2pzH)_2]ClO_4$ (1b) towards Ag(I) species to give the$[\ Pt_2Ag_2]$ cluster, 4

The reactions of $[Pt(C^C^*)(3,5\text{-}Me_2pzH)_2]ClO_4$ (**1b**) with $AgClO_4$ in 1:1 molar in the presence of NEt_3 resulted in the elimination of the two acidic hydrogens and their replacement by Ag(I) centers with the subsequent formation of the tetranuclear cluster $[\{Pt(C^C^*)(3,5\text{-}Me_2pz)_2Ag\}_2]$ (**4**) (see Exp Section and Figures S19-S22). The absence of absorptions due to N-H bonds in the IR and the FAB+ mass spectra are in agreement with the single-crystal X-ray structure of **4** (see Figure 2, Table S1).

As can be seen, **4** is a tetranuclear $[Pt_2Ag_2]$ cluster comprised of two "$Pt(C^C^*)(3,5\text{-}Me_2pz)_2Ag$" subunits joined through Ag-N bonds and Ag···Ag interactions. Each

subunit consists of one "Pt(C^C*)(3,5-Me_2pz)$_2$Ag" fragment with a 3,5-Me_2pz bridging the Pt and Ag centers located in close proximity.

Figure 2. Molecular structure of compound **4**. Ellipsoids are drawn at their 50% probability level and hydrogen atoms were omitted for clarity. Selected bond lengths (Å) and angles (º): Pt-Ag, 3.2626(5); Ag-Ag#1, 3.2171(9); N4-Ag-N6#1, 169.2(2).

The angle between the Pt-Ag vector and the platinum coordination plane (35.62º) in addition to the Pt-Ag distance are indicative of Pt→Ag dative bonds.[16] This Pt-Ag distance is shorter than those observed in the related tetranuclear clusters $[Pt_2Ag_2(N^C)_2(Me_2pz)_4]^{0,\,2+}$ (N^C = ppy-, dfppy, bpy, $d_{Pt\text{-}Ag} > 3.4$ Å).[9a] The Ag center of each subunit completes its coordination environment with a N of a 3,5-Me_2pz belonging to the other Pt subunit with N-Ag-N angles close to 180º. Both silver centers interact with each other, with the Ag···Ag distance being 3.2171(9) Å, quite similar to those observed in other pyrazolate-bridged Pt/Ag clusters which is indicative of argentophilic interactions.[9a, 10, 16]

In line with the X-ray structure, the ^{1}H NMR spectrum of freshly solutions of **4** in CD_2Cl_2 (rt, Figure S19; 183 K Figure S20) shows the expected resonances for half of the molecule with two sets of signals corresponding to the inequivalent pyrazolates of one "Pt(C^C*)(3,5-Me_2pz)$_2$" unit. Upon interaction with the silver center, all resonances shift upfield except that of H7 that moves to downfield and shows a moderately

reduction of the ^{3}J(H,Pt) coupling constant from 59.2 Hz in **1b** to 51.2 Hz in **4**. This is in line with the existence of the Pt−M interactions in solution.[17] Also, ^{195}Pt NMR spectrum of **4** supports this statement, showing a signal at −3753 ppm in CD_2Cl_2 solution at 183 K (Figure S22) which is downfield shifted when compared to that of **1b** (−3920 ppm, 298 K), in agreement with reported results.[9b, 18]

Optical properties

UV-Vis spectra and Theoretical calculations

The absorption spectra of compounds **1a**–**1c**, **2b** and **3b** in CH_2Cl_2 (10^{-4} M) solutions (Table S2, Figure S23 and 3 for **1a**) exhibit intense absorptions at $\lambda < 300$ nm ($\varepsilon \geq 10^4$ M^{-1} cm^{-1}), normally attributed to intraligand (^{1}IL) transitions of the NHC ligand. They also display absorption bands at *ca*. 315 nm ($\varepsilon\sim 10^3$ M^{-1} cm^{-1}) with a shoulder in the range 340-360 nm. The absorptions of **1b** and **1c** at $\lambda > 300$ nm are very similar to each other while that of **1a** appears slightly red shifted (Figure S23 (a)) indicating subtle differences because of the change in the counteranion. When comparing the perchlorate derivatives (**1b-3b,** Figure S23 (b)), we observed a great similarity in the lower-energy region of their spectra. Thus, it seems that the RpzH ligands do not much affect the absorption nor participate in the low energy transitions.

The absorptions at $\lambda > 300$ nm do not change either in CH_2Cl_2 at concentrations ranging from 10^{-3} to 10^{-6} M (see Figure S24 for **2b**) nor in different solvents (CH_2Cl_2, 2-MeTHF and MeOH) at low concentration (10^{-4} M) (see Table S2 and Figure S25 for **1b**) indicating these absorptions to be due to transitions in the molecular species with no significant aggregation occurring within this concentration range and the absence of significant solvatochromism.

Diffuse reflectance spectra of powdery samples of **1a–1c**, **2a**, **2b** **3a** and **3b** (Figure S26) show no significant differences with respect to those observed in CH_2Cl_2 solution

in the range 200-400 nm. However, unlike them, they show weak and similar absorptions in the range 400 – 450 nm, which could be related with the intermolecular interactions absent in diluted solutions. Like in solution, the changes of both, the RpzH and the counteranion neither seem to have significant effect in the absorption properties in solid state at room temperature. When comparing the UV-vis spectra of **4** with that of its precursor, **1b**, a lower energy band at ~ 350 nm appeared (see Figure S27 (a)). Diffuse reflectance spectrum of **4** resembles the UV-Vis one obtained from a freshly solution of **4** in CH_2Cl_2 (see Figure S27). Therefore, according to this and the NMR experiments, the Pt_2Ag_2 core is most likely kept in solution.

The time-dependent density functional theory (TD-DFT) results (Figure 3 and Table 1; Figure S28, and Tables S3-S6 in SI) indicate that the HOMO → LUMO transition is the only contribution to the calculated spin-allowed transition from S_0 to S_1 (see Table 1). The lowest energy calculated absorptions (S_1) fit well with the experimental ones (Figures 3 and S28).

Hence, the UV-Vis spectra of these compounds can be interpreted by focusing on the analysis of their molecular orbitals (MO) obtained by the DFT calculations, which show that the highest occupied molecular orbital (HOMO) and the lowest unoccupied molecular orbital (LUMO) are mainly centered on the NHC ligand (63-72% H; 76-85% L) and the Pt (27-33% H; 14-25% L) with a marginal contribution of the ancillary ligands (< 5%), which confirm that the Cl and the pyrazol ligands show barely any involvement in the crucial transition processes.

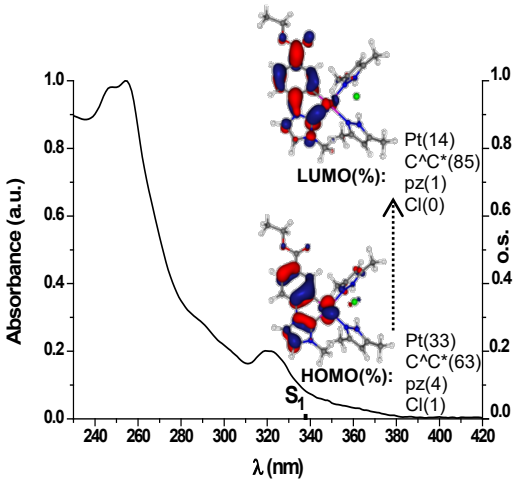

Figure 3. UV-vis absorption spectrum, calculated transition in CH_2Cl_2 (bars) and calculated molecular orbitals for **1a**

Also, the neutral or cationic nature of the compounds (**1a** *vs* **1b**) appears to have very little effect on them. In view of the nature of the HOMO and LUMO, the lowest energy absorption in all compounds has been attributed to a metal-perturbed intraligand charge transfer transition on the N-heterocyclic carbene (ILCT [(NHC)]) with a small metal-to-ligand charge transfer contribution (MLCT).

Table 1. S1 states calculated by TD-DFT in solution of CH_2Cl_2

Comp.	λexc (calc.)/nm	o.s.	Transition(%)	Assignment
1a	337.8	0.0084	H →L (95)	ILCT, MLCT
1b	337.3	0.0064	H → L (96)	ILCT, MLCT
2b	334.8	0.0051	H → L (96)	ILCT, MLCT
3b	334.6	0.0059	H → L (96)	ILCT, MLCT

Luminescence spectra

The emission spectra of compounds **1a–3a, 1b, 3b** and **1c** in rigid matrix (10^{-5} M CH_2Cl_2 solution at 77 K) or in poly(methyl methacrylate) (PMMA) films at 5 wt% are quite similar. They show highly structured emissions (λ_{max} ~ 455 nm) with vibronic spacings [~ 1450 cm^{-1}] corresponding to the C=C / C=N stretches of the cyclometalated NHC ligands (see Figure 4 for **1b** Figure S29 and Table 2) with long emission lifetime decays (14 – 22 μs), typical of phosphorescent Pt(II) systems. The emission energies are neither affected by the nature of the RpzH ligand nor the anion and are very similar to those observed in related compounds containing the same "(C^C*)Pt" fragment.[4b, 4c]

Thus, taking into account all these data and the TD-DFT calculations, these phosphorescent emissions are originated from the monomeric species and assigned mainly to intraligand charge transfer on the N-heterocyclic carbene (^{3}ILCT [(NHC)]).

Powdery solid samples of **1a–3a, 1b-3b** and **1c** display bright blue emissions at 298 K (see Table 2 and Figure S30 for **1a-1c**, **1b-3b**) exhibiting band profiles and lifetimes that resemble those obtained in rigid matrix of CH_2Cl_2.

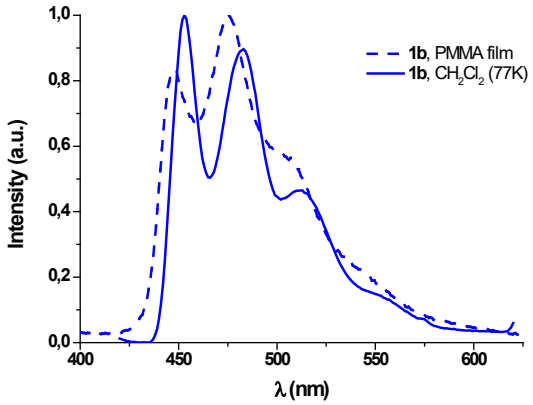

Figure 4. Normalized emission spectra of **1b**. Picture of **1b** taken under UV light (365 nm).

As can be observed, the emission of powdery solid samples is slightly blue shifted when the counter anion is Cl^- (**1a**) instead of ClO_4^- (**1b**) or PF_6^- (**1c**). Luminescent mononuclear bis-pyrazole Pt(II) compounds are very scarce in the literature. When comparing the emission properties of these mononuclear species with those of other bis-pyrazole compounds [Pt(fppz)(3,5-Me_2pzH)$_2$]Cl [fppzH = 3-(trifluoromethyl)-5-(2-pyridyl)pyrazole)][13c] and [(C^N)Pt(pz)$_2$BEt_2] [C^N = (2-(2,4-difluorophenyl)pyridyl],[19] some similarities concerning the emission profiles and lifetimes were found, but the Photoluminescence Quantum Yields (PLQY) of our complexes in PMMA films (5 wt%) are far more higher with values up to 100%.

As observed in Table 2 and Figure 5, all emissions except that of **1a** render QY values of 100% and Commission Internationale de L'Éclairage (CIE) coordinates of (0.15,

0.22) which are very close to the desirable ones for blue emitters (0.15, 0.15).[2i] These mononuclear bis-pyrazole compounds are amongst the best blue light emitters of Pt(II) with QY values in PMMA film higher than the reported ones: [Pt(C^C*)(acac)] (Φ = 0.86,[2d] 0.90[2e]), [Pt(C*^C^C*)Cl] (Φ = 0.32[2j]) and [Pt(C^X-L^L')] [C^X = phenyl methyl imidazole; L^L' = phenoxy pyridine, Φ = 0.58; L^L' = carbazolyl pyridine, Φ = 0.89; C^X = phenyl pyrazole; L^L' = carbazolyl pyridine, Φ = 0.85].[2i] The emission efficiency of **1b, 2b** and **1c** in PMMA films is in the range, but even larger than those of the related compounds [Pt(R-C^C*)(acac)] (QY = 0.98 R= CN, 0.93 R=CO_2Et in 5 wt% PMMA films).[4d] Undoubtely, the presence of an electro-withdrawing substituent in the *para* position to the carbene fragment guarantees a high efficiency. In these bis-pyrazole compounds, the likely perpendicular disposition of the RpzH with respect to the Pt coordination plane will hinder the intermolecular Pt···Pt interactions, a fact that seems to lower the emission efficiency, as we could observe in previous work.[4d]

Table 2. Photophysical data for **1a**–**3a**, **1b**–**3b, 1c** and **4**.

Comp	**Media (T/K)**	**λ_{ex}(nm)**	**λ_{em} (nm)**	**τ(μs)**[b]	**ϕ**[c]
1a	CH_2Cl_2[a](77)	322	454$_{max}$, 486, 514	14.0	
	PMMA	360	449, 476$_{max}$, 504		0.66
	Film				
	Solid (298)	362	448, 475$_{max}$, 505, 540$_{sh}$	17.7	

2a[d]	CH_2Cl_2[a](77)	325	453_{max}, 481, 520	14.9	
	Solid (298)	363	447, 477_{max}, 509, 546_{sh}		
3a[d]	CH_2Cl_2[a](77)	325	454_{max}, 486, 518	12.3	
	Solid (298)	362	452, 483_{max}, 515, 550_{sh}		
1b	CH_2Cl_2[a](77)	319	453_{max}, 483, 512, 553_{sh}	21.6	
	PMMA Film	360	447, 475_{max}, 505,540_{sh}		1.00
	Solid (298)	360	463, 489_{max}, 517, 560_{sh}	13.4	0.33
2b	CH_2Cl_2[a](77)	319	456_{max}, 488, 517	18.2	
	PMMA Film	360	446, 475_{max}, 500		0.99
	Solid (298)	370	458, 487_{max}, 516	10.1	
3b[e]	CH_2Cl_2[a](77)	316	451_{max}, 481, 511, 555_{sh}	19.7	
	Solid (298)	366	460, 484_{max}, 515	15.9	
1c	CH_2Cl_2[a](77)	319	454_{max}, 482, 512_{sh}	21.2	
	PMMA Film	360	455, 478_{max}, 512		1.00
	Solid (298)	370	461, 487_{max}, 518_{sh}	12.9	
4	CH_2Cl_2[a](77)	340	453_{max}, 484, 512_{sh}	8.4	
	Solid (298)	360	454, 483_{max}, 510	6.4	0.51

a = 10^{-5} M; *b*= measurements at λ_{max}; *c* = PMMA films in Ar atmosphere; d= the dynamic equilibrium in solution hindered the PMMA film to be prepared conveniently for photophysical measurements. In CH_2Cl_2 at 77K does not experiment any change at least for 24h. e= QY in PMMA film has not been measured because **3b** evolves partially to [{Pt(C^C*)(μ-pz)}$_2$] in CH_2Cl_2 at r.t.

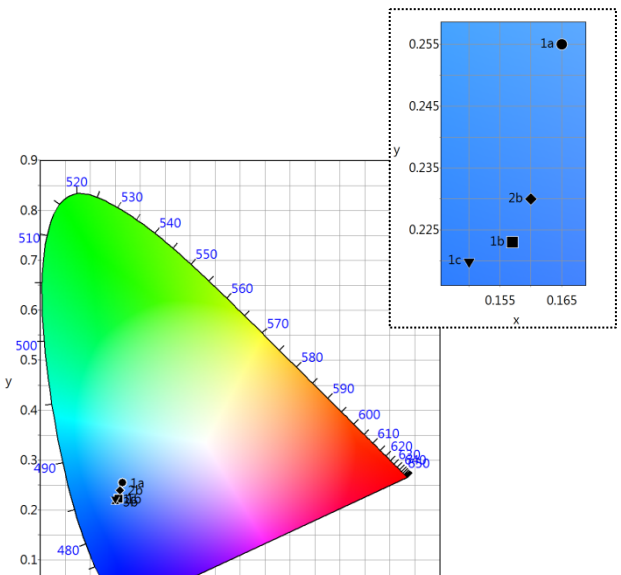

Figure 5. CIE 1931 chromaticity diagram with the (x, y) positions of the emissions of **1a-1c** and **2b** in PMMA films.

The most significant feature of **4**, regarding its emissive behavior, is the blue shift of the emission band of powdery solid in relation to that of its precursor, **1b** (see Figure S31). This reflects the formation of the Pt→Ag dative bond since the electron density of the Pt center decreases upon bonding to $Ag^{+,}$ lowering the energy of HOMO.[20] Likewise, there is a considerable reduction of the emission lifetime and an increase of the QY values from 0.33 (**1b**) to 0.55 (**4**) in powdery solid samples. According to this and in line with similar compounds,[9] this emission has been assigned to a mixed ^{3}IL/^{3}MLCT emissive state.

Conclusions

The availability of the cyclometalated N-heterocyclic carbene compound [{Pt(C^C*)(μ-Cl)}$_2$](**A**) (HC^C* = 1-(4-(ethoxycarbonyl)phenyl)-3-methyl-1*H*-imidazol-2-ylidene) as starting material allowed to get the new bis-pyrazole complexes [Pt(C^C*)(RpzH)$_2$]X, as chloride (Cl^-), perchlorate (ClO_4^-) or hexafluorophosphate (PF_6^-) salts. Their behavior in CH_2Cl_2 solution at room temperature illustrates the higher basicity of the 3,5-Me$_2$pzH with respect to 4-MepzH and pzH and the dependence of the stability of these compounds on the RpzH and X nature. Then, among the chloride compounds, just [Pt(C^C*)(3,5-Me$_2$pzH)$_2$Cl](**1a**) is stable in CH_2Cl_2 solution at r.t. while the 4-MepzH and pzH derivatives coexist with the corresponding [Pt(C^C*)(R-pzH)Cl](**B**) species in

a dynamic equilibria which can be avoided by lowering the temperature to *ca.* 220 K. Regarding the perchlorate compounds, $[Pt(C^C^*)(pzH)_2]ClO_4$ partially evolves to give $[Pt(C^C^*)(\mu\text{-}pz)\}_2]$ and free pzH in solution at r.t. Experimental data and TD-DFT calculations showed that the nature of both, the anion and the substituent of the ancillary ligands (RpzH) do not deeply affect the blue emission of these compounds which can be mainly assigned to intraligand charge transfer transitions on the N-heterocyclic carbene (^{3}ILCT [(NHC)]). The perchlorate and hexafluorophosphate derivatives (**1b**, **2b**, **1c**) are fully efficient blue-light emitters with QY up to 100% in PMMA films. However, the efficiency of the chloride compound (**1a**) decreases to 66%. Compound **1b** has been proved to behave as a useful synthon to reach the $[Pt_2Ag_2]$ cluster, **4**, by the replacement of the acidic H of 3,5-Me_2pzH by Ag^+.

Experimental Section

Information describing materials, instrumental methods used for characterization, photophysical and spectroscopic studies, computational details concerning TD-DFT calculations, and X-ray structures are provided in the Supporting Information. All chemicals were used as supplied unless stated otherwise. The starting material $[\{Pt(\mu\text{-}Cl)(C^C^*)\}_2]$ (**A**) was prepared following the literature procedure.[4b] 3,5-Me_2pzH, 4-MepzH, $AgClO_4$ were purchased from Sigma-Aldrich. pzH was purchased from MERCK and $AgPF_6$ was purchased from fluorochem.

Synthesis of [Pt(C^C*)(3,5-Me_2pzH)$_2$Cl] (1a)

3,5-Me_2pzH (46.5 mg, 0.48 mmol) was added to a suspension of **A** (100.0 mg, 0.11 mmol) in acetone (30 mL) at room temperature and the mixture stirred for 24 h. Then the solvent was removed under reduced pressure. The residue was treated with hexane/Et_2O (20/1 mL) and the resulting solid was filtered, and washed with hexane to give **1a** as a yellow solid. Yield: 133.4 mg (61%). ^{1}H NMR (400 MHz, CD_2Cl_2, 25ºC):

δ = 14.5 (s br, 1H; NH), 14.3 (s br, 1H; NH), 7.72 (dd, ^{3}J(H9,H10) = 8.1, ^{4}J (H9,H7) = 1.8, 1H; H9), 7.48 (d, ^{3}J(H2,H3) = 2.1, 1H; H2), 7.15 (d, ^{3}J (H10,H9) = 8.1, ^{4}J(H,Pt) = 23.5, 1H; H10), 6.92 (d, ^{4}J(H9,H7) = 1.8, ^{3}J(H,Pt) = 57.5, 1H; H7), 6.80 (d, ^{3}J(H3,H2) = 2.1, 1H; H3), 6.05 (s, 1H, H4'; 3,5-Me_2pzH), 5.98 (s, 1H, H4''; 3,5-Me_2pzH), 4.22 (q, ^{3}J(H,H) = 7.1, 2H, CH_2; CO_2Et), 2.97 (s, 3H; H4), 2.38, 2.37, and 2.31 (s, 12H, Me; 3,5-Me_2pzH), 1.29 (t, ^{3}J(H,H) = 7.1, 3H, CH_3; CO_2Et). $^{13}C\{^{1}H\}$ NMR (101 MHz, CD_2Cl_2, 25ºC): δ = 166.9 (s; *C*O_2Et), 155.5 (s; C1), 151.5 (s; C5), 149.6, 148.9, 143.3 and 143.1 (s, 4C, C3', C3'', C5', C5''; 3,5-Me_2pzH), 135.6 (s; C7), 129.0 and 127.4 (s, 2C; C6 and C8), 127.1 (s; C9), 123.0 (s; C3), 115.9 (s; C2), 110.9 (s; C10), 106.2 (s, C4'; 3,5-Me_2pzH), 106.0 (s, C4''; 3,5-Me_2pzH), 61.0 (s, CH_2; CO_2Et), 35.3 (s; C4), 14.9 and 14.7 (s, 2C, Me; 3,5-Me_2pzH), 14.5 (s, CH_3; CO_2Et), 11.3 (s, 2C, Me; 3,5-Me_2pzH). $^{195}Pt\{^{1}H\}$ NMR (85.6 MHz, CD_2Cl_2, 25ºC): δ = –3889.6 (s). IR (ATR, cm^{-1}): ν =2917 (m, br, NH), 1708 (m, C=O). MS (MALDI+): m/z 616.3 $[M]^+$. Λ_M ($5\cdot10^{-4}$ M acetone solution): 9.53 Ω^{-1} cm^2 mol^{-1}. Elemental analysis calcd (%) for $C_{23}H_{29}ClN_6O_2Pt$: C 42.37, H 4.48, N 12.89; found: C 42.01, H 4.29, N 12.88.

Synthesis of [Pt(C^C*)(4-MepzH)$_2$Cl] (2a)

Complex **2a** was synthesized following the same procedure used for **1a** with 4-MepzH (22 μL, 0.27 mmol) and **A** (54 mg, 0.06 mmol). **2a**, yellow solid. Yield: 35.0 mg (64%). ^{1}H NMR (400 MHz, CD_2Cl_2, –40ºC): δ = 14.7 (s br, 1H; NH), 14.5 (s br, 1H; NH), 7.70 (dd, ^{3}J(H9,H10) = 8.1, ^{4}J(H9,H7) = 1.7, 1H; H9), 7.63 (s, 1H; 4-MepzH), 7.61 (s, 1H; 4-MepzH), 7.53 (s, 1H; 4-MepzH), 7.51 (s, 1H; 4-MepzH), 7.47 (d, ^{3}J(H2,H3) = 1.8, 1H; H2), 7.14 (d, ^{3}J(H10,H9) = 8.1, 1H; H10), 6.91 (d, ^{4}J(H7,H9) = 1.7, ^{3}J(H, Pt) = 51.3, 1H; H7), 6.72 (d, ^{3}J(H3,H2) = 1.8, 1H; H3),4.15 (q, ^{3}J(H,H) = 7.1, 2H, CH_2; CO_2Et), 2.92 (s, 3H; H4), 2.12 (s, 3H, Me; 4-MepzH), 2.05 (s, 3H, Me; 4-MepzH), 1.15 (t, ^{3}J(H,H) = 7.1, 3H, CH_3; CO_2Et). $^{195}Pt\{^{1}H\}$ NMR (85.6 MHz, CD_2Cl_2, -40ºC): δ =

–3874.1 (s). IR (ATR, cm^{-1}): ν = 2926 (m, br, NH), 1703 (m, C=O). MS (MALDI+): m/z 506.2 $[Pt(C^C*)(4\text{-}MepzH)]^+$. Elemental analysis calcd (%) for $C_{21}H_{25}ClN_6O_2Pt$: C 40.42, H 4.04, N 13.47; found: C 40.31, H 3.84, N 13.42.

Synthesis of [Pt(C^C*)(pzH)$_2$Cl] (3a)

Complex **3a** was synthesized following the same procedure used for **1a** with pzH (20.6 mg, 0.30 mmol) and **A** (61.3 mg, 0.07 mmol). **3a**, yellow solid. Yield: 31.4 mg (60%). ^{1}H NMR (400 MHz, CD_2Cl_2, –60ºC): δ= 15.0 (s br, 1H; NH), 14.9 (s br, 1H; NH), 7.89 (s, 1H; pzH), 7.85 (s, 1H; pzH), 7.75 (s, 1H; pzH), 7.73 (s, 1H; pzH), 7.68 (dd, ^3J(H9,H10) = 8.1, ^4J(H9,H7) = 1.4, 1H; H9), 7.57 (s, 1H; H2), 7.20 (d, ^3J(H10,H9) = 8.1, 1H; H10), 6.83 (d, ^4J(H7,H9) = 1.4, ^3J(H,Pt) = 50.5, 1H; H7), 6.64 (s,1H; H3), 6.51 (s, 1H; pzH), 6.44 (s, 1H; pzH), 4.13 (q, ^3J(H,H) = 6.9, 2H, CH_2; CO_2Et), 2.83 (s, 3H; H4), 1.23 (t, ^3J(H,H) = 6.9, 3H, CH_3; CO_2Et). ^{195}Pt{^{1}H} NMR (85.6 MHz, CD_2Cl_2, -60ºC): δ = –3880.8 (s). IR (ATR, cm^{-1}): ν = 2975 (m, br, NH), 1700 (m, C=O). MS (MALDI+): m/z 492.2 $[Pt(C^C*)(pzH)]^+$. Elemental analysis calcd (%) for $C_{19}H_{21}ClN_6O_2Pt$: C 38.29, H 3.55, N 14.10; found: C 37.97, H 3.42, N 13.71.

Synthesis of [Pt(C^C*)(3,5-Me$_2$pzH)$_2$]ClO$_4$ (1b)

$AgClO_4$ (45.5 mg, 0.22 mmol) was added to a stirred suspension of **A** (100.0 mg, 0.11 mmol) in acetone (50 mL) in the dark at room temperature. After 2 h of reaction, 3,5-Me_2pzH (42.2 mg, 0.44 mmol) was added to the mixture and allowed to react for 16.5 h in the darkness. Then, the resulting suspension was filtered through Celite and the solvent was removed under reduced pressure. The residue was treated with hexane/Et_2O (20/1 mL) and filtered to give **1b** as a pale yellow solid. Yield: 110.7 mg (71 %). ^{1}H NMR (400 MHz, CD_2Cl_2, 25ºC): δ = 11.8 (s br, 1H; NH), 11.6 (s br, 1H; NH), 7.75 (dd, ^3J(H9,H10) = 8.1, ^4J(H9,H7) = 1.8, 1H; H9), 7.36 (d, ^3J(H2,H3) = 2.2, 1H; H2), 7.07 (d, ^3J(H10,H9) = 8.1, 1H; H10), 6.86 (d, ^3J(H3,H2) = 2.2, 1H; H3), 6.84 (d, ^4J(H7,H9) =

1.8, ^{3}J(H,Pt) = 59.2, 1H; H7), 6.13 (s, 1H, H4'; 3,5-Me_2pzH), 6.06 (s, 1H, H4''; 3,5-Me_2pzH), 4.22 (q, ^{3}J(H,H) = 7.1, 2H, CH_2; CO_2Et), 3.06 (s, 3H; H4), 2.41, 2.37, 2.36 and 2.34 (s, 12H, Me; 3,5-Me_2pzH), 1.29 (t, ^{3}J(H,H) = 7.1, 3H, CH_3; CO_2Et). $^{13}C\{^{1}H\}$ NMR (101 MHz, CD_2Cl_2, 25ºC): δ = 166.7 (s; *C*O_2Et), 155.0 (s; C1), 151.0 (s; C5), 150.2, 150.0 and 144.4 (s, 4C, C3', C3'', C5', C5''; 3,5-Me_2pzH), 135.6 (s; C7), 128.2 (s; C8), C6 is not detected, 127.5 (s; C9), 123.0 (s; C3), 115.7 (s; C2), 110.8 (s; C10), 106.8 (s, C4'; 3,5-Me_2pzH), 106.6 (s, C4''; 3,5-Me_2pzH), 61.1 (s, CH_2; CO_2Et), 35.5 (s; C4), 14.7 (s, 1C, Me; 3,5-Me_2pzH), 14,8 (s, 1C, Me; 3,5-Me_2pzH), 14.5 (s; CH_3, CO_2Et), 11.3 (s, 2C; Me, 3,5-Me_2pzH). $^{195}Pt\{^{1}H\}$ NMR (85.6 MHz, CD_2Cl_2, 25ºC): δ = –3920.1 (s). IR (ATR, cm^{-1}): ν = 3140 (m, br, NH), 1668 (m, C=O), 1060, 620 (s, ClO_4). MS (MALDI+): m/z 616.2 $[M]^+$. Λ_M ($5\cdot10^{-4}$ M acetone solution): 103.5 Ω^{-1} cm^2 mol^{-1}. Elemental analysis calcd (%) for $C_{23}H_{29}ClN_6O_6Pt$: C 38.58, H 4.08, N 11.73; found: C 38.49, H 4.05, N 11.80.

Synthesis of [Pt(C^C*)(4-MepzH)$_2$]ClO$_4$ (2b)

$AgClO_4$ (45.5 mg, 0.22 mmol) was added to a stirred suspension of **A** (100.0 mg, 0.11 mmol) in acetone (50 mL) in the dark at room temperature. After 3 h, 4-MepzH (36 µL, 0.44 mmol) was added to the mixture and allowed to react for 14 h in the darkness. Then, the resulting suspension was filtered through Celite and the solvent was evaporated to dryness. The residue was treated with hexane/Et_2O (20/1 mL) and filtered, to give **2b** as a pale yellow solid. Yield: 133.5 mg (89 %). ^{1}H NMR (400 MHz, CD_2Cl_2, 25ºC): δ = 12.2 (s br, 1H; NH), 12.0 (s br, 1H; NH), 7.76 (dd, ^{3}J(H9,H10) = 8.1, ^{4}J(H9,H7) = 1.9, 1H; H9), 7.65 (s, 1H, H3''; 4-MepzH), 7.64 (s, 1H, H3'; 4-MepzH), 7.59 (s, 1H, H5''; 4-MepzH), 7.54 (s, 1H, H5'; 4-MepzH), 7.35 (d, ^{3}J(H2,H3) = 2.1, 1H; H2), 7.07 (d, ^{3}J(H10,H9) = 8.1, 1H; H10), 6.90 (d, ^{4}J(H7,H9) = 1.7, ^{3}J(H7,Pt) = 58.5, 1H; H7), 6.85 (d, ^{3}J(H3,H2) = 2.1, 1H; H3), 4.22 (q, ^{3}J(H,H) = 7.1, 2H, CH_2; CO_2Et),

3.01 (s, 3H; H4), 2.16 (s, 3H, Me'; 4-MepzH), 2.11 (s, 3H, Me''; 4-MepzH), 1.28 (t, ^{3}J(H,H) = 7.1, 3H, CH_3; CO_2Et). $^{13}C\{^{1}H\}$ NMR (101 MHz, CD_2Cl_2, 25ºC): δ = 166.7 (s; *C*O_2Et), 154.2 (s; C1), 151.4 (s; C5), 140.7(s, C5''; 4-MepzH), 140.6 (s, C5'; 4-MepzH), 135.6 (s; C7), 131.1 (s, C3''; 4-MepzH), 130.8 (s, C3'; 4-MepzH), 127.8 (s; C9), 127.5 (s, 2C; C6 and C8), 123.0 (s; C3), 118.6 (s, C4''; 4-MepzH), 118.3 (s; C4'; 4-MepzH), 115.7 (s; C2), 111.0 (s; C10), 61.2 (s, CH_2; CO_2Et), 35.8 (s; C4), 14.5 (s, CH_3; CO_2Et), 9.1 (s, 2C, Me' and Me''; 4-MepzH). $^{195}Pt\{^{1}H\}$ NMR (85.6 MHz, CD_2Cl_2, 25ºC): δ = –3915.6 (s). IR (ATR, cm^{-1}): ν = 3137 (m, NH), 1655 (m, C=O), 1077, 623 (s, ClO_4). MS (MALDI+): m/z 588.3 $[M]^+$. Λ_M ($5\cdot10^{-4}$ M acetone solution): 103.8 Ω^{-1} cm^2 mol^{-1}. Elemental analysis calcd (%) for $C_{21}H_{25}ClN_6O_6Pt$: C 36.66, H 3.66, N 12.22; found: C 36.29, H 3.66, N 12.35.

Synthesis of [Pt(C^C*)(pzH)$_2$]ClO$_4$ (3b)

Complex **3b** was synthesized following the same procedure used for **2b** with $AgClO_4$ (46.2 mg, 0.22 mmol), **A** (101.4 mg, 0.11 mmol) and pzH (30.0 mg, 0.44 mmol). **3b**, white solid. Yield: 114.0 mg (78 %). ^{1}H NMR (400 MHz, CD_3OD, 25ºC): δ = 8.02 (m, 2H; pzH), 7.93 (d, ^{3}J(H,H) = 1.9, 1H; pzH), 7.80 (m, 2H; H2 and H (pzH)), 7.75 (dd, ^{3}J(H9,H10) = 8.2, ^{4}J (H9,H7) = 1.7, 1H; H9), 7.31 (d, ^{3}J(H10,H9) = 8.2, 1H; H10), 7.22 (d, ^{3}J (H3,H2) = 2.1, 1H; H3), 7.01 (d, ^{4}J(H7,H9) = 1.7, ^{3}J(H,Pt) = 57.0, 1H; H7), 6.61 (m, 2H, H4' and H4''; pzH), 4.23 (q, ^{3}J(H,H) = 7.1, 2H, CH_2; CO_2Et), 3.15 (s, 3H; H4), 1.30 (t, ^{3}J(H,H) = 7.1, 3H, CH_3; CO_2Et). $^{13}C\{^{1}H\}$ NMR (101 MHz, CD_3OD, 25ºC): δ = 168.0 (s; *C*O_2Et), 155.0 (s; C1), 152.9 (s; C5), 141.8 (s, 1C; pzH), 141.4 (s, 1C; pzH), 136.3 (s; C7), 132.7 (s, 1C; pzH), 132.6 (s, 1C; pzH), 128.4 (s; C9), 128.7 and 127.7 (s; C6 and C8), 124.4 (s; C3), 116.7 (s; C2), 111.7 (s; C10), 108.5 (s, 1C; pzH), 108.1 (s, 1C; pzH), 61.8 (s, CH_2; CO_2Et), 35.6 (s; C4), 14.5 (s, CH_3; CO_2Et). $^{195}Pt\{^{1}H\}$ NMR (85.6 MHz, CD_3OD, 25ºC): δ = –3923.7 (s). IR (ATR, cm^{-1}): ν= 3134 (m, br, NH),

1662 (m, C=O), 1086, 622 (s, ClO_4). MS (ESI+): m/z 560.1 $[M]^+$. Λ_M ($5\cdot10^{-4}$ M acetone solution): 100.6 Ω^{-1} cm^2 mol^{-1}. Elemental analysis calcd (%) for $C_{19}H_{21}ClN_6O_6Pt\cdot2H_2O$: C 32.79, H 3.62, N, 12.08; found: C 33.1, H 3.48, N 12.10.

Synthesis of [Pt(C^C*)(3,5-Me$_2$pzH)$_2$]PF$_6$ (1c)

$AgPF_6$ (44.0 mg, 0.17 mmol) was added to a stirred suspension of **A** (80.0 mg, 0.09 mmol) in acetone (50 mL) in the darkness at room temperature. After 3 h, 3,5-Me_2pzH (33.79 mg, 0.35 mmol) was added to the mixture and allowed to react for 14 h in the darkness. Then, the resulting suspension was filtered through Celite and the solvent was evaporated to dryness. The residue was treated with hexane/Et_2O (20/1 mL) and filtered to give **1c** as a pale yellow solid. Yield: 60.0 mg (45 %). ^{1}H NMR (300 MHz, CD_2Cl_2, 25ºC): δ = 11.0 (s br, 1H; NH), 10.9 (s br, 1H; NH), 7.76 (dd, ^3J(H9,H10) = 8.1, ^4J(H9,H7) = 1.5, 1H; H9), 7.37 (d, ^3J(H2,H3) = 1.9, 1H; H2), 7.08 (d, ^3J(H10,H9) = 8.1, ^4J(H,Pt) = 22.2, 1H; H10), 6.88 (d, ^3J(H3,H2) = 1.9, 1H; H3), 6.86 (s, ^3J(H,Pt) = 58.9, 1H; H7), 6.14 (s, 1H, H4'; 3,5-Me_2pzH), 6.07 (s, 1H, H4''; 3,5-Me_2pzH), 4.22 (q, ^3J(H,H) = 7.1, 2H, CH_2; CO_2Et), 3.07 (s, 3H; H4), 2.40, 2.34 (s, 12H, Me; 3,5-Me_2pzH), 1.29 (t, ^3J(H,H) = 7.1, 3H, CH_3; CO_2Et). ^{195}Pt{^{1}H} NMR (85.6 MHz, CD_2Cl_2, 25ºC): δ = –3931.3 (s). IR (ATR, cm^{-1}): ν = 3150 (m, NH), 1675 (m, C=O), 831, 555 (s, PF_6). MS (MALDI+): m/z 616.2 $[M]^+$. Λ_M ($5\cdot10^{-4}$ M acetone solution): 134.8 Ω^{-1} cm^2 mol^{-1}. Elemental analysis calcd (%) for $C_{23}H_{29}F_6N_6O_2PPt$: C 36.27, H 3.84, N 11.04; found: C 36.09, H 3.80, N 11.02.

Synthesis of [{Pt(C^C*)(3,5-Me$_2$pz)Ag}$_2$] (4)

To a solution of **1b** (150 mg, 0.21 mmol) in methanol (10 mL) was added $AgClO_4$ (45 mg, 0.21 mmol) and excess of NEt_3 (0.5 mL, 3.58 mmol). The solution was stirred for 1 h at r.t. in the dark. The resulted yellow precipitate was collected, washed with methanol, and dried in vacuum. Yield 116 mg (78%). ^{1}H NMR (400 MHz, CD_2Cl_2,

25ºC): δ = 7.63 (dd, ^{3}J(H9,H10) = 8.1, ^{4}J(H9,H7) = 1.7, 2H; H9), 7.18 (d, ^{3}J(H2,H3)= 2.0, 2H; H2), 7.15 (d, ^{4}J(H7,H9) = 1.7, ^{3}J(H,Pt) = 51.2, 2H; H7), 6.88 (d, ^{3}J(H10,H9) = 8.1, 2H; H10), 6.57 (d, ^{3}J(H3,H2) = 2.0, 2H; H3), 6.01 (s, 2H, H4'; 3,5-Me_2pz), 5.78 (s, 2H, H4'; 3,5-Me_2pz), 4.21 (m, 4H; CH_2, CO_2Et), 2.41 (s, 6H; H4), 2.22 (s, 6H, Me; 3,5-Me_2pz), 2.21 (s, 6H, Me; 3,5-Me_2pz), 2.03 (s, 6H, Me; 3,5-Me_2pz), 1.70 (s, 6H, Me; 3,5-Me_2pz), 1.28 (t, ^{3}J (H,H) = 7.1, 6H, CH_3; CO_2Et). $^{13}C\{^{1}H\}$ NMR (101 MHz, CD_2Cl_2, –90ºC): δ = 166.8 (s; *C*O_2Et), 159.0 (s; C1), 151.5 (s; C5), 148.2, 147.0, 146.1 (s; 3,5-Me_2pz), 137.1 (s; C7), 134.5 (s; C6), 126.3 (s; C8), 125.8 (s; C9), 122.5 (s; C3), 113.8 (s; C2), 109.6 (s; C10), 102.8 (s, C_4; 3,5-Me_2pz), 102.6 (s, C4'; 3,5-Me_2pz), 60.8 (s, CH_2; CO_2Et), 33.6 (s, C4), 14.2, 14.1, 14.0 (s, CH_3; CO_2Et and 3,5-Me_2pz), 13.6, 13.2 (s, Me; 3,5-Me_2pz). $^{195}Pt\{^{1}H\}$ NMR (85.6 MHz, CD_2Cl_2, –90ºC):δ = –3753.5 (s). IR (ATR, cm^{-1}): ν = 1701 (m, C=O). MS (MALDI+): m/z 627.2 $[M–(3,5\text{-}Me_2pz)_2]^{2+}$; 1349.3 $[M–(3,5\text{-}Me_2pz)]^{+}$; 1553.4 $[M + Ag]^{+}$. Elemental analysis calcd (%) for $C_{46}H_{54}Ag_2N_{12}O_4Pt_2$: C 38.24, H 3.77, N 11.63; found: C 38.00, H 3.63, N 11.54.

Acknowledgements

This work was supported by the Spanish Ministerio de Economía y Competitividad (MINECO)/FEDER (Project CTQ2015-67461-P led by Dr. Babil Menjón) and by the Gobierno de Aragón and Fondo Social Europeo (Grupo Consolidado E21: Química Inorgánica y de los Compuestos Organometálicos led by Dr. José M. Casas). The authors thank the Centro de Supercomputación de Galicia (CESGA) for generous allocation of computational resources.

REFERENCES

[1] a) Z. Chen, L. Wang, S. Su, X. Zheng, N. Zhu, C.-L. Ho, S. Chen, W.-Y. Wong, *ACS Appl. Mater. Interfaces* **2017**, *9*, 40497-40502; b) I. Omae, *Coord. Chem. Rev.*

2016, *310*, 154-169; c) T. von Arx, A. Szentkuti, T. N. Zehnder, O. Blacque, K. Venkatesan, *J. Mater. Chem. C* **2017**, *5*, 3765-3769; d) T. Strassner, *Acc. Chem. Res.* **2016**, *49*, 2680-2689.

[2] a) M. Bachmann, D. Suter, O. Blacque, V. K., *Inorg. Chem.* **2016**, *55*, 4733−4745; b) H. Leopold, U. Heinemeyer, G. Wagenblast, I. Münster, T. Strassner, *Chem. Eur. J.* **2016**, *22*, 1 - 12; c) A. Tronnier, G. Wagenblast, I. Münster, T. Strassner, *Chem. Eur. J.* **2015**, *21*, 12881-12884 and references therein; d) Z. M. Hudson, C. Sun, M. G. Helander, Y. L. Chang, Z. H. Lu, S. N. Wang, *J. Am. Chem. Soc.* **2012**, *134*, 13930-13933; e) Y. Unger, D. Meyer, O. Molt, C. Schildknecht, I. Münster, G. Wagenblast, T. Strassner, *Angew. Chem., Int. Ed.* **2010**, *49*, 10214-10216; f) J. Lee, H. F. Chen, T. Batagoda, C. Coburn, P. I. Djurovich, M. E. Thompson, S. R. Forrest, *Nat. Mater.* **2016**, *15*, 92-99; g) G. J. Li, T. Fleetham, J. Li, *Adv. Mater.* **2014**, *26*, 2931-2936; h) T. Fleetham, G. J. Li, L. L. Wen, J. Li, *Adv. Mater.* **2014**, *26*, 7116-7121;) iX. C. Hang, T. Fleetham, E. Turner, J. Brooks, J. Li, *Angew. Chem. Int. Ed.* **2013**, *52*, 6753-6756; j) T. Fleetham, Z. X. Wang, J. Li, *Org. Electron.* **2012**, *13*, 1430-1435.

[3] A. F. Rausch, L. Murphy, J. A. G. Williams, H. Yersin, *Inorg. Chem.* **2011**, *51*, 312-319.

[4] a) S. Fuertes, H. Garcia, M. Peralvarez, W. Hertog, J. Carreras, V. Sicilia, *Chem. - Eur. J.* **2015**, *21*, 1620-1631; b) S. Fuertes, A. J. Chueca, M. Perálvarez, P. Borja, M. Torrell, J. Carreras, V. Sicilia, *ACS App. Mat. Interfaces* **2016**, *8*, 16160-16169; c) S. Fuertes, A. J. Chueca, L. Arnal, A. Martín, U. Giovanella, C. Botta, V. Sicilia, *Inorg. Chem.* **2017**, *56*, 4829-4839; d) S. Fuertes, A. J. Chueca, A. Martín, V. Sicilia, *Cryst. Growth Des.* **2017**, *17*, 4336-4346.

[5] K. Sakai, Y. Tomita, T. Ue, K. Goshima, M. Ohminato, T. Tsubomura, K. Matsumoto, K. Ohmura, K. Kawakami, *Inorg. Chim. Acta* **2000**, *297*, 64-71.

[6] F. K. Keter, J. Darkwa, *Biometals* **2012**, *25*, 9-21.

[7] a) S. Kuwata, T. Ikariya, *Chem. Commun.* **2014**, *50*, 14290-14300; b) Y. Nakahara, T. Toda, A. Matsunami, Y. Kayaki, S. Kuwata, *Chem. Asian J.* **2018**, *13*, 73-80; c) Y. Suna, Y. Himeda, E. Fujita, J. T. Muckerman, M. Z. Ertem, *ChemSusChem* **2017**, *10*, 4535-4543.

[8] J. Forniés, S. Fuertes, A. Martín, V. Sicilia, E. Lalinde, M. T. Moreno, *Chem. Eur. J.* **2006**, *12*, 8253-8266.

[9] a) K. Nishihara, M. Ueda, A. Higashitani, Y. Nakao, Y. Arikawa, S. Horiuchi, E. Sakuda, K. Umakoshi, *Dalton Trans* **2016**, *45*, 4978-4982; b) M. Ueda, S. Horiuchi, E. Sakuda, Y. Nakao, Y. Arikawa, K. Umakoshi, *Chem. Commun.* **2017**, *53*, 6405-6408.

[10] S. Akatsu, Y. Kanematsu, T.-a. Kurihara, S. Sueyoshi, Y. Arikawa, M. Onishi, S. Ishizaka, N. Kitamura, Y. Nakao, S. Sakaki, K. Umakoshi, *Inorg. Chem.* **2012**, *51*, 7977-7992.

[11] K. Umakoshi, K. Saito, Y. Arikawa, M. Onishi, S. Ishizaka, N. Kitamura, Y. Nakao, S. Sakaki, *Chem. Eur. J.* **2009**, *15*, 4238-4242.

[12] S. Fuertes, A. J. Chueca, V. Sicilia, *Inorg. Chem.* **2015**, *54*, 9885-9895.

[13] a) T. Steiner, *J. Phys. Chem. A* **1998**, *102*, 7041-7052; b) A. Martín, *J. Chem. Educ.* **1999**, *76*, 578-583; c) S.-Y. Chang, J.-L. Chen, Y. Chi, Y.-M. Cheng, G.-H. Lee, C.-M. Jiang, P.-T. Chou, *Inorg. Chem.* **2007**, *46*, 11202-11212; d) P. N. Fonteh, F. K. Keter, D. Meyer, I. A. Guzei, J. Darkwa, *J. Inorg. Biochem.* **2009**, *103*, 190-194.

[14] W. J. Geary, *Coord. Chem. Rev.* **1971**, *7*, 81-122.

[15] L. M. Epstein, E. S. Shubina, *Coord. Chem. Rev.* **2002**, *231*, 165-181.

[16] J. Fornies, V. Sicilia, J. M. Casas, A. Martín, J. A. López, C. Larraz, P. Borja, C. Ovejero, *Dalton Trans.* **2011**, *40*, 2898-2912 and references therein.

[17] a) S. Jamali, Z. Mazloomi, S. M. Nabavizadeh, D. Milic, R. Kia, M. Rashidi, *Inorg. Chem.* **2010**, *49*, 2721-2726; b) G. J. Arsenault, C. M. Anderson, R. J. Puddephatt, *Organometallics* **1988**, *7*, 2094-2097.

[18] a) D. E. Janzen, L. F. Mehne, D. G. VanDerveer, G. J. Grant, *Inorg. Chem.* **2005**, *44*, 8182-8184; b) T. Yamaguchi, F. Yamaguchizaki, T. Ito, *J. Am. Chem. Soc.* **2001**, *123*, 743-744; c) S. Fuertes, C. H. Woodall, P. R. Raithby, V. Sicilia, *Organometallics* **2012**, *31*, 4228-4240.

[19] B. Ma, J. Li, P. I. Djurovich, M. Yousufuddin, R. Bau, M. E. Thompson, *J. Am. Chem. Soc.* **2005**, *127*, 28-29.

[20] a) A. Diez, E. Lalinde, M. Teresa Moreno, *Coord. Chem. Rev.* **2011**, *255*, 2426-2447; b) M. C. Moret, P. J. Chen, *J. Am. Chem. Soc.* **2009**, *131*, 5675-5690; c) J. Forniés, S. Ibañez, A. Martin, M. Sanz, J. R. Berenguer, E. Lalinde, J. Torroba, *Organometallics* **2006**, *25*, 4331-4340.

Entry for the Table of Contents

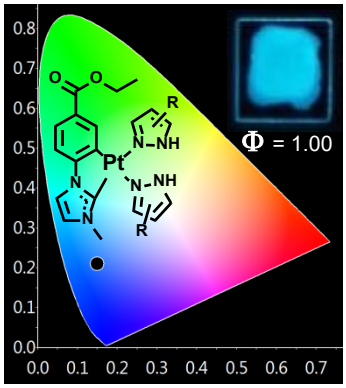

Pyrazole & NHC's, the winner mix for Pt(II)

Pyrazoles combined with N-Heterocyclic carbenes cyclometallated to a Pt(II) center have been proven to produce fully efficient blue light emitters with QY of 100%.